Title
Caged Cumate Enables Proximity-Dependent Control Over Gene Expression

Journal
ChemBioChem, 22(14)

ISSN
1439-4227

Authors
Love, Anna C
Tran, Sabrina H
Prescher, Jennifer A

Publication Date
2021-07-15

DOI
10.1002/cbic.202100158

Peer reviewed

HHS Public Access

Author manuscript

Chembiochem. Author manuscript; available in PMC 2023 January 23.

Published in final edited form as:

Chembiochem. 2021 July 15; 22(14): 2440–2448. doi:10.1002/cbic.202100158.

Caged Cumate Enables Proximity-Dependent Control over Gene Expression

Anna C. Love[a], **Sabrina H. Tran**[b], **Jennifer A. Prescher**[a,c,d]

[a]Department of Chemistry, University of California, Irvine, 1120 Natural Sciences II, Irvine, CA 92697 (USA)

[b]Department of Biological Sciences, University of California, Irvine, 5120 Natural Sciences II, Irvine, CA 92627 (USA)

[c]Department of Molecular Biology and Biochemistry, University of California, Irvine, 3205 McGaugh Hall, Irvine, CA 92697 (USA)

[d]Department of Pharmaceutical Sciences, University of California, Irvine, 101 Theory, Ste. 101, Irvine, CA 92697 (USA).

Abstract

Cell-cell interactions underlie diverse physiological processes yet remain challenging to examine with conventional imaging tools. Here we report a novel strategy to illuminate cell proximity using transcriptional activators. We repurposed cumate, a small molecule inducer of gene expression, by caging its key carboxylate group with a nitrile. Nitrilase-expressing activator cells released the cage, liberating cumate for consumption by reporter cells. Reporter cells comprising a cumate-responsive switch expressed a target gene when in close proximity to the activator cells. Overall, this strategy provides a versatile platform to image and potentially manipulate cellular interactions over time.

Graphical Abstract

jpreche@uci.edu .

Supporting information for this article is given via a link at the end of the document.

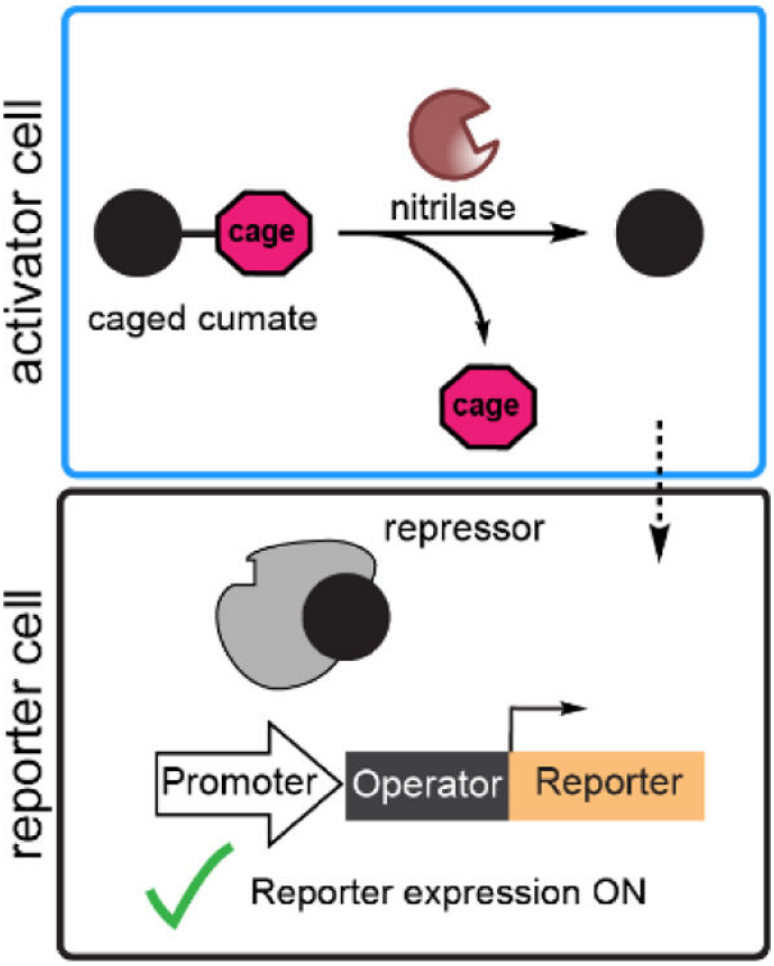

A new strategy for visualizing cellular interactions was developed based on the cumate genetic switch. Nitrile-caged cumate released by activator cells induces gene expression in neighboring reporter cells.

Keywords

caged probe; gene transcription; cumate; cellular contact; imaging

Introduction

Cell-cell interactions are ubiquitous in organisms and can potentiate disease, but methods to selectively visualize and ultimately control them are lacking.[1–3] Current strategies rely on imaging with fluorescent proteins[4–8] or enzymatic labeling.[9–12] While useful, many of these methods are not generalizable to multiple cell types or provide only short-lived signals. More versatile approaches that are amenable to a wider range of cellular interactions and readouts are necessary.

Strategies that rely on small molecule activation are particularly attractive.[10] Small molecules are readily tunable and can trigger a variety of biological processes through

molecular recognition.[13] Indeed, caged small molecules have been coopted to monitor different cellular interactions in complex biological settings.[14–16] These probes are outfitted with molecular masks that block activity.[17] The masks can be selectively removed by complementary enzymes. Caged probes have historically been used to activate imaging probes and release therapeutics in cells of interest.[17–20] In these cases, the uncaging enzymes and biological targets are located in the same cell.[21] Caged probes can be used to report on cellular interactions if the uncaging enzyme is expressed in one cell (i.e., an "activator" cell) and the binding partner for the released probe is expressed in a different cell (i.e., a "reporter" cell). The administration of the caged probe elicits a proximity-dependent response. How far the response can be visualized is dependent on the solubility and permeability of the uncaged small molecule, as well as the concentration administered.

The caged probe strategy hinges on the selectivity of the uncaging enzyme and cage pair. The cage must block key functionality for biological recognition, and be selectively removed by the enzyme. In the ideal case, the caged probe is readily bioavailable and rapidly released by orthogonal (non-endogenous) enzymes in the host. Cages that meet these criteria include nitro-aromatic groups that are selectively reduced by nitroreductase, along with galactose moieties that are selectively removed by β-galactosidase.[22–23] Indeed, these probes have been used for decades to liberate drugs and other cargos at defined tissues.[23–27] More recently, they have been repurposed to illuminate cellular interactions at static time points.[18, 28] In one example, galactose-caged luciferin was used to image tumor-immune cell interactions. Robust emission was observed when T cells expressing β-galactosidase and tumor cells expressing firefly luciferase were co-localized. [29]

Despite such successes, the toolbox of enzyme-cage pairs for probing cell proximity remains small. Only a few pairs have been used extensively in mammalian systems. Most also provide only transient readouts of cellular interactions. Unless samples are recorded continuously, many of the interactions can be missed. More permanent readouts can be achieved using alternative small molecules. In a recent example from the Sellmyer lab, caged trimethoprim was used to tune protein degradation in a cell interaction-dependent manner.[15] Activator cells expressing nitroreductase released trimethoprim, which diffused into reporter cells to stabilize proteins fused to degradation domains. Proximity-dependent signal was observed over longer periods of time, and the strategy was applicable to controlling not just imaging probes, but also signaling agents and other outputs.

We aimed to expand upon the need for more modular and long-lived reporters of cell proximity. Our focus was on manipulating molecules that control transcription. Transcriptional activation can provide long-lived (e.g., multi-day) readouts of cell interactions, ensuring that more transient events are not missed.[30–32] This concept underlies some technologies for probing cell contact, including the synNotch platform developed by the Lim lab.[33] SynNotch releases transcriptional activators upon cell-cell engagement, driving the expression of reporter genes.[34–35] While impactful, synNotch requires multi-subunit proteins that can be difficult to translate to multiple cell types.

Herein, we combine the desirable features of small molecule uncaging with the longevity of transcriptional inducers for effective and general tracking of cellular interactions. We

capitalized on small molecule regulation of gene expression in prokaryotes,[36] where metabolites regulate pathways by binding and releasing repressor proteins from DNA. Downstream genes can thus be transcribed and control metabolic flux. A variety of these pathways have been coopted as inducible expression systems in mammalian cells.[37] We focused on engineering one such platform, the cumate genetic switch,[38] to report on cellular interactions (Figure 1A). We identified an effective cage for cumate and verified its stability *in vitro* and *in cellulo*. We further characterized the enzyme-mediated removal of cage *in vitro* and in culture with activator cells. Finally, we showed that the caged cumate genetic switch platform could report on mixtures of interacting cells. This approach is the first example of a repressor-based system for monitoring cell proximity. The method features simple small molecules, easy-to-engineer gene expression pathways, and proteins with no localization requirements. Thus, it should be generally applicable to a variety of cell interaction studies.

Results and Discussion

The cumate genetic switch features a repressor protein that binds an operator sequence. If the operator is situated between the promoter and gene of interest, the bound repressor blocks transcription. Cumate binding induces a conformational change in the repressor, releasing it from the DNA and allowing transcription to occur. Transcription could thus be regulated in a proximity-dependent manner if cumate was selectively released by one cell and used to “turn-on” gene expression in a neighboring cell (Figure 1A). Building on this idea, we sought a caged version of cumate that is inactive until liberated by activator cells (Figure 1B). Activator cells expressing a suitable uncaging enzyme would release cumate, enabling it to diffuse into nearby reporter cells and drive reporter gene production (Figure 1C-D).

We selected the cumate genetic switch for several reasons. First, this system controls terpene degradation in bacteria and the components are orthogonal to mammalian transcriptional machinery.[39] The cumate system has also been successfully used in a variety of mammalian cells and is not activated by other endogenous small molecules.[38] Second, repressor platforms are well-known staples of genetic circuits and can be tailored to elicit varying levels of gene transcription. [40] End users can thus tune the expression of the desired gene using defined doses of cumate. Last, cumate itself is cell permeable, soluble in aqueous solutions at biologically relevant concentrations, and able to induce a response in reporter cells that persists for days, allowing the dynamics of cellular interactions to be studied over time.

At the outset, we required a cage/uncaging enzyme pair to use with the cumate genetic switch. Cumate (**2**) is a simple molecule, with limited functionality available to manipulate.

However, biological studies revealed that the carboxylate is key to repressor protein binding and could serve as a target for modification.[39] We also desired an enzyme with fast uncaging kinetics such that minimal and transient cell contacts could be captured. We further desired an uncaging enzyme not present in the gut microbiota to limit off-target cumate release in future animal studies. With these criteria in mind, we selected nitrilase as the

uncaging enzyme. Nitrilase converts both alkyl and aryl nitrile moieties to carboxylates and acts on a variety of substrates.[41–43] Nitrilase has been previously used for targeted uncaging of amino acids in mammalian cells,[44] but has yet to be widely used for cell-specific cargo delivery. The enzyme is also not expressed by endogenous gut bacteria, mitigating concerns of off-target release *in vivo*.

To evaluate the cage/enzyme pair for cell studies, we designed a nitrile-caged version of cumate (compound **1**, Figure 1B). This analog comprises a nitrile in place of the critical carboxylate group. Since nitriles are distinct from carboxylates in terms of their steric and electronic properties, we hypothesized that the cage would be sufficient to render compound **1** biologically inactive. We also hypothesized that the probe would be stable in aqueous solutions, as hydrolysis of nitriles typically requires harsh conditions.[45] Indeed, when compound **1** (1 mM) was incubated in buffer over 7 d at 37 ºC, no hydrolysis was observed (Figures 2A, S1).

We next assayed whether cumate could be released from the caged compound using purified nitrilase. We selected the enzyme from *Rhodococcus rhodochrous* (*Rr*NIT) since it has been previously employed in mammalian cells.[44] Further, *Rr*NIT has been shown to exhibit substrate promiscuity and high activity.[46] The conversion of nitrile **1** to cumate was evaluated via HPLC (Figure 2B, S2). Stock solutions of **1** (1 mM) were incubated with purified *Rr*NIT over time and compared to synthetic standards. Approximately half of the sample was uncaged after 4 h, whereupon conversion stalled (likely due to loss of enzyme activity in 10% acetonitrile). The addition of fresh enzyme resulted in full uncaging. We further verified the activity of the isolated enzyme via ammonia release with a standard absorbance assay.[47] *Rr*NIT exhibited dose-dependent uncaging of compound **1** (Figure S3)

With a suitable uncaging enzyme identified, we assessed the cumate switch *in cellulo*. As noted earlier, the platform involves cumate binding to CymR, lifting it from CuO and enabling downstream gene transcription (Figure 3A). We engineered cells to stably express a CymR-eGFP fusion protein. We also generated a reporter plasmid comprising DsRed under the control of the CuO operator (Figure 3B). We verified that the eGFP fusion did not impede CymR binding to the CuO operator (Figure S4). We then transfected the CuO-DsRed reporter plasmid into cells stably expressing CymR-eGFP and dosed in various levels of cumate. After 3 d, cells were analyzed via flow cytometry. Gratifyingly, a dose dependent increase in DsRed expression was observed. The highest concentration of cumate (1 mM) provided the most robust response (Figure 3C-D, S5), but significant switching was observed with as little as 5 μM compound (Figure S6). DsRed production was detected in untreated cells, likely due to leaky expression associated with inducible platforms.[48–49] However, the signal turn-on observed with cumate is sufficient for many imaging experiments. In cases where a larger dynamic range is necessary, the operator and repressor sequences can be further engineered.

We also assayed DsRed expression over time. The CuO-DsRed reporter construct was similarly transfected into the CymR-eGFP cell line, and samples were treated with cumate. Cells were analyzed via flow cytometry and DsRed expression was found to peak on the last day of analysis, day 3 (Figure S7). Thus, all subsequent flow cytometry analyses

were performed 3 d post cumate administration. We further measured the length of cumate exposure necessary for robust DsRed expression. As shown in Figure S8, cumate (100 μM) incubation times of 4h resulted in significant reporter gene expression.

After validating the genetic switch platform in cells, we examined the robustness of the caged probe. We verified that caged compound **1** did not cross-react with CymR, producing undesirable background signal. CymR-eGFP cells were transfected with the CuO-DsRed reporter construct, and treated with various doses of compound **1**. Cells were incubated for 3 d, then DsRed expression was analyzed using flow cytometry (Figure 4). No increase in DsRed expression was observed, suggesting that the caged compound is unable to bind CymR. We next assayed whether *Rt*NIT could uncage compound **1** *in cellulo. Rt*NIT-expressing cells were incubated with **1**, and media from the cultures was then transferred to prepared reporter cells. Successful uncaging and downstream activity was observed, with DsRed expression levels comparable to reporter cells incubated with cumate itself (Figure S9).

We further assessed the kinetics of caged cumate release *in cellulo*. *Rt*NIT cells (or control HEK cells) were incubated with caged probe **1** for 15 min-24 h. Media from the cultures was then transferred to reporter cells expressing CymR-eGFP and CuO-DsRed. After 3 d, DsRed expression was analyzed via flow cytometry. A significant increase in DsRed expression was observed after only 15 min of caged compound exposure to *Rt*NIT-expressing cells (Figure 5A, S10). A similar level of signal induction was observed when the reporter cells were treated with cumate (**2**) itself. Further, the difference in DsRed expression was not statistically different between cells exposed for 15 min versus 24 h. The fast uncaging kinetics of nitrilase with probe **1** will be useful for a variety of caged probe studies.

We next determined the minimum threshold of cells that the caged probe must encounter to achieve full uncaging. Varying numbers of *Rt*NIT (1,000–100,000 cells) or control HEK cells were treated with caged probe **1** for 15 min. Media from the cultures was transferred to reporter cells as before, and DsRed expression was analyzed via flow cytometry. Excitingly, only 1,000 activator cells were required to rapidly uncage probe **1**. The levels of DsRed expression achieved were on par with the addition of cumate itself (Figure 5B, S11). These results suggest that the caged cumate strategy could be applicable to studying transient cellular contacts or contacts that take place with small populations of activator cells.

Putting it all together, we aimed to show that the cumate switch can report on interacting cells. Reporter populations nearest the activator eGFP-*Rt*NIT cells would be expected to exhibit higher levels of DsRed signal. To test this hypothesis, we plated activator cells expressing CymR and CuO-DsRed with reporter eGFP-*Rt*NIT cells at defined distances using biocompatible stencils.[50] Cells were either seeded together or 10 mm apart, then incubated with caged compound **1**. Media was replaced after 8 h, and cells were further incubated for 3 d to allow for gene expression. Flow cytometry was used to quantify DsRed expression in the reporter cells. Co-cultures of the activator and reporter cells resulted in robust DsRed expression, while physically separated cells showed a reduction in signal, on par with the negative control (Figure 6A). Smaller distances and longer incubation times resulted in equally robust reporter expression among co-cultured and separated cells (Figure

S12), since cumate is easily diffusible. More stringent readouts on distance were achieved when a low dose of caged cumate was administered (Figure 6B, S13, and Videos 1-4). However, the lower dose inevitably resulted in reduced reporter induction. The tradeoff between robust fluorescence and distance dependency must be considered when applying the caged cumate system in static cultures. It is likely that both high signal induction and stringent readouts on distance can be achieved in environments with interstitial flow (e.g., *in vivo*).

Conclusion

We developed a strategy for monitoring cellular interactions over time with a caged probe and the cumate genetic switch platform. We designed a simple, yet stable nitrile-caged cumate probe that can be readily converted to the corresponding carboxylic acid by nitrilase. Cumate can induce robust changes in gene expression. Cumate uncaging is also rapid, with only low levels of nitrilase required. We further showed that cumate release can be coopted to report on cell proximity. Nitrilase-expressing (activator) cells can locally liberate cumate for use by cumate-responsive reporter cells. The transcriptional turn-on in reporter cells is robust and long-lived, enabling even transient interactions to be readily “recorded“ and imaged post-contact.

The strategy reported here is applicable to imaging and manipulating a variety of cellular interactions. The platform makes use of simple small molecules and gene expression pathways, that can be readily tuned to provide modular readouts. The fluorescent protein reporter can be replaced with any gene of interest, enabling production of a variety of reporters and other outputs. For example, inducing expression of a signaling protein regulatory element could modulate cell function in an interaction-dependent manner.

While generalizable, the cumate platform relies on diffusion of a small molecule. This aspect must be tightly controlled for the strategy to report on direct cell contacts. Thus, the cumate system lacks the high specificity of synNotch and other intracellularly released transcriptional activators. More precise readouts can potentially be achieved, though, by tuning the permeability of the probes, or engineering CymR to exhibit improved affinity for cumate. Additional gains in specificity are likely to come *in vivo*, where flow and turbidity minimize excess compound in the milieu.[10] These and other parameters will be explored in future iterations of the caged cumate platform.

Experimental Section

General information

Q5 DNA polymerase, all restriction enzymes, and all associated buffers were purchased from New England BioLabs. dNTPs were purchased from Thermo Fisher Scientific. Luria-Bertani medium (LB) was purchased from Genesee Scientific. Cuminyl nitrile caged probe **1** was purchased from Alfa Aesar. All plasmids and primer stocks were stored at 4 °C unless otherwise noted. Primers were purchased from Integrated DNA Technologies (IDT) and plasmids were sequenced by Genewiz. Sequencing traces were analyzed using Benchling. Nanopure water was used for all biological methods unless otherwise noted.

General cloning methods

Polymerase chain reaction (PCR) was used to isolate all genes of interest. The genes were ligated into destination vectors via Gibson assembly.[51] Primer melting temperatures (T_m) were determined using the NEB T_m calculator. All PCR reactions were performed in a BioRad C3000 Thermocycler using the following conditions: 1) 95 °C for 3 min, 2) 95 °C for 30 s, 3) T_m of primers for 30 s, 4) 72 °C for 3 min, repeat steps 2–4 twenty times, then 72 °C for 5 min, and hold at 12 °C until retrieval from the thermocycler. Gibson assembly conditions were 50 ºC for 60 min and held at 12 ºC until retrieval from the thermocycler. Ligated plasmids were transformed into the TOP10 strain of *E. coli* using the heat shock method. After incubation at 37 °C for 18–24 h, colonies were picked and subjected to colony PCR to check for successful gene insertion. Select colonies were expanded overnight in 3 mL LB broth supplemented with ampicillin (100 μg/mL) or kanamycin (100 μg/mL). DNA was extracted from colonies using a Zymo Research Plasmid Mini-prep Kit.

General cell culture methods

HEK293 cells (HEK, ATCC) and stable cells lines derived from HEK293 cells were cultured in complete media: DMEM (Corning) containing 10% (v/v) fetal bovine serum (FBS, Life Technologies), penicillin (100 U/mL), and streptomycin (100 μg/mL, Gibco). Cell lines stably expressing CymR-eGFP, CymR, or eGFP-*Rt*NIT were generated via transfection of HEK293 with Lipofectamine 2000 and the following three plasmids: AAVS1 donor plasmid containing the relevant gene of interest, Cas9 (Addgene #41815), and AAVS1 sgRNA (Addgene #53370). Transfected cells were further cultured with puromycin (20 μg/mL) to preserve gene incorporation. Cells were incubated at 37 °C in a 5% CO_2 humidified chamber. Cells were serially passaged using trypsin (0.25% in HBSS, Gibco).

General fluorescence imaging

Fluorescence microscopy images were acquired on a Keyence BZ-X800 microscope using a 4X or 40X objective. Appropriate filters were used to image both DsRed and eGFP expression. Exposure times were selected below threshold for camera saturation. Exposure times for eGFP were set at 1/8.5 s and exposure times for DsRed were set at 1/20 s. Images were analyzed using Fiji. For magnified cells, exposure times were 1/8.5 s for set eGFP markers and 1/80 s for DsRed markers.

General transient transfection methods

Cells were seeded 24–48 h prior to transfection in tissue culture treated, Corning 6-well plates (250,000 cells plated per well) or 12-well plates (150,000 cells per well). When the cultures reached 75–80% confluency (~1–2 d post plating), cells were transfected were with the CuO-DsRed reporter plasmid using Lipofectamine 2000. Cells were then analyzed 24–48 h post transfection.

General flow cytometry methods

Cells were treated with 1X citrate saline solution (0.015 M sodium citrate, 0.135 M potassium chloride) for 5 min at 37 °C. Cells were then transferred to Eppendorf tubes and pelleted (500*g*, 4 min) using a tabletop centrifuge (Thermo Fischer Sorvall Legend

Micro 17). The resulting supernatants were discarded, and cells were washed with PBS (2 × 400 μL). Cells were then immediately analyzed on a Novocyte flow cytometer (ACEA BioSciences Inc). Live cells were gated and, in some cases (e.g., CymR-eGFP cells transfected with CuO-DsRed reporter construct), eGFP+ cells were further gated. For each sample, 10,000 events were collected on either the “Live cell” gate, the “eGFP+” gate, or the “eGFP-” gate (see Figures S13 and S14 for raw plots). DsRed fluorescence was analyzed and quantified using NovoExpress software (ACEA Biosciences Inc).

General data analysis methods

For all bar graphs, standard errors of the mean were calculated using n=3 or n=9 replicates. To determine statistical significance, unpaired t-tests were performed using GraphPad Prism 6, and the following notation was used: ****$p < 0.0001$, ***$p < 0.001$, **$p < 0.01$, *$p < 0.05$.

RrNIT protein expression and purification

*Rr*NIT expression and purification was performed similarly to the procedure reported by Luo, *et al.*[46] In brief, a pET plasmid encoding NIT with a C-terminal His tag[52] was transformed into chemically competent *E. coli* BL21 cells. Transformants were plated on agar plates containing kanamycin (50 μg/mL). Single colonies were grown in 50 mL of LB with kanamycin (50 μg/mL) overnight. The starter cultures were added to 1 L of LB with kanamycin (50 μg/mL) and allowed to grow at 220 rpm at 37 °C to OD600 = 0.8. IPTG was added to a concentration of 1 mM, and cultures were grown at 23 °C for 24 h at 220 rpm. Cultures were then centrifuged at 4000 *g* for 8 min and the resulting pellets were resuspended in 40 mL of lysis buffer (20 mM Tris HCl, 150 mM NaCl, 0.5% v/v Tween-20, pH 7.8) with protease inhibitor (PMSF, 0.1 mM). Cells were lysed with sonication and centrifuged (13,000 rpm, 1 h at 4°C). The supernatants were then applied to prepared Ni-NTA columns for 30 min. The flow through was collected in each case, and three washes were performed with wash buffer (50 mM Na_3PO_4, 20 mM imidazole, pH 7.8). Four elutions were performed with elution buffer (50 mM Na_3PO_4, 500 mM imidazole, pH 7.8). The elution fractions were combined and dialyzed for 24 h in dialysis buffer (50 mM Na_3PO_4, pH 7.8). Proteins were concentrated via spin column (GE Healthcare, VivaSpin, 30 kDa MWCO). Protein concentrations were determined via absorbance measurements (280 nm) using a JASCO V-730 Spectrophotometer with a quartz cuvette. Molar extinction coefficients were calculated using the ExPASy ProtParam tool.

Absorbance assay for purified nitrilase activity

*Rr*NIT activity was confirmed using an established absorbance assay.[47] In brief, a stock solution of caged probe **1** was prepared in 100% ethanol (100 mM). The solution (23 μL) was diluted with phosphate buffer (PBS, 10 mM) in a 96-well plate (Corning). Purified *Rr*NIT (15–90 μg) was then added to each well such that the final volumes per well totaled 230 μL. A standard curve of ammonium chloride (0–11 mM) in PBS (10 mM) was also prepared on the same 96-well plate. The plate was covered and incubated at 37 ºC for 18 h. The next day, a solution of *o*-phthalaldehyde in MeOH (200 mg/mL) was prepared and diluted (1:100) with sodium tetraborate buffer (15 mM, pH 9.5) immediately prior to use.

This solution (100 μL) was combined with each sample from the 96-well plate (50 μL), along with additional DMSO (140 μL) and trichloroacetic acid (50 μL, 10% w/v). Next, each sample was further diluted (1:2) into DMSO and incubated at room temperature for 10 min. Absorbance values (675 nm) were then recorded using a Tecan Spark multimode microplate reader. Assays were performed in triplicate and data were analyzed using GraphPad Prism 6. The concentration of ammonia in each case was calculated using the standard curve.

HPLC uncaging assay

Stocks of **1** and **2** (250 mM in MeCN with 0.1% formic acid) were diluted to 1 mM using 10 mM ammonium bicarbonate buffer with 10% MeCN. Samples of **1** were incubated with purified *Rt*NIT enzyme (90 μg). The final volume of each reaction was 500 μL. Reactions were incubated at 37 ºC for 1–24 h, and enzymes were precipitated via addition of 500 μL cold MeOH wih 1% formic acid. Reactions were filtered and the filtrate was further analyzed. Reactions incubated for 24 h were treated with an additional 90 μg *Rt*NIT and incubated for an additional 1 h at 37 ºC. Synthetic standards for **1** and **2** were prepared in 50:50 H_2O:MeCN with 0.1% formic acid. The standards and reaction samples were analyzed using an Agilent Technologies 1260 Infinity Series II HPLC equipped with a diode array detector. Separations were performed using an Agilent Poroshell C18 column (eluting with 50–100% MeCN in H_2O containing 0.1% formic acid over 20 min). The flow rate was set at 0.2 mL/min. Raw traces were exported as .CSV files and analyzed in GraphPad Prism 6. Data were min-max normalized prior to plotting.

In cellulo analysis of cumate genetic switch

HEK293 cells or cells stably expressing CymR-eGFP/CymR were transfected with the CuO-DsRed reporter plasmid. Cells were trypsinized 24 h post transfection and transferred to 12-well clear plates (75,000 cells/well). Cumate (**2**, 0–1 mM) was added and cells were incubated for 3 d at 37 ºC in a humidified incubator. Cells were then imaged and analyzed via flow cytometry for DsRed expression. HEK293 cells expressing CymR-eGFP and untransfected HEK293 cells were used to establish the appropriate gates.

Time course analysis of cumate genetic switch

Cells were prepared as described above. Compound **2** (100 μM) was added and incubated with cells for (0–24 h). Media was then removed from the culture and cells were washed with PBS (1 × 800 μL) to remove excess **2**. Fresh media was added and cells were incubated an additional 24 h prior to flow cytometry analysis.

In cellulo analysis of caged cumate

Cells were prepared as described above. Twenty-four hours post transfection, cells were added to a 12-well dish and incubated with **1** or **2** (0–1 mM). Cells were incubated for 3 d and then analyzed via flow cytometry for DsRed expression.

In celluo uncaging of cumate probe

HEK293 cells or cells expressing eGFP-*Rt*NIT were added to a 12-well plate (100,000 cells/well unless otherwise specified). Caged probe **1** (1 mM) was added to each well,

and cells were incubated for 24 h (unless otherwise specified). Media was then transferred to CymR-eGFP cells transfected with the CuO-DsRed reporter plasmid (reporter cells) described above. Reporter cells were incubated with media for 3 d prior to flow cytometry analysis.

Stencil experiments to determine proximity dependence

HEK293 cells and CymR-expressing cells were plated in 6-well plates and transfected with the CuO-DsRed reporter plasmid. Biocompatible stencils[50] were used to separate the cells. Prior to cell addition, the stencils were sterilized with 100% ethanol in 3-inch petri dishes (10 mm stencils) or 12-well plates (3–7 mm stencils) and allowed to dry uncovered in a biosafety cabinet for several hours. The stencil wells were then coated with Matrigel (Corning) according to the manufacturer's instructions. Transfected cells and eGFP-*Rt*NIT cells were immediately plated (50 μL/well, 75,000 cells/well for petri dishes, 30 μL/well, 30,000 cells/well for 12-well plates) and allowed to settle over 3–4 h. Stencils were then removed using sterilized forceps, and media (2 mL for petri dishes, 1 mL for 12-well plates) was slowly added to each well to avoid lifting cells. Compounds **1** (experimental wells) or **2** (positive control) were added (1 mM) to the wells. For negative controls, no compound was added. For petri dish samples, media was removed after 8 h, cells were rinsed with 1 mL media, and fresh media was added. Cells were then incubated for an additional 3 d prior to imaging and analysis via flow cytometry. For 12-well plate samples, **1** or **2** (10 μM) were added and Z-stack images were captured every hour using a Keyence BZ-X800 microscope and time-lapse image capture program. The only channel acquired was DsRed, and the exposure time was set to 1/25 s. DsRed positive cells were counted in CellProfiler.[53] For supplemental videos, images were analyzed and videos were created using FIJI. Workflow for image editing was as follows: Images>Images to Stack>Images>Z Project>Max Intensity. Max Intensity stacks were saved, and videos were compiled from these images.

CellProfiler analysis

CellProfiler was downloaded online from the website www.cellprofiler.org. The center images from the acquired Z-stacks were compiled. The following modules were included in the CellProfiler pipeline used to count individual cells: Images, ColorToGray, IdentifyPrimaryObjects, ExportToSpreadsheet. The "ColorToGray" module was used to color the red input .tiff images to grayscale as required to run the IdentifyPrimaryObjects module. The IdentifyPrimaryObjects module named "cells" as objects with diameters between 1 and 40 pixels. All other objects in the image were discarded as well as objects touching the border of the image. Lastly, the ExportToSpreadsheet module was used to export the number of cells counted to an Excel spreadsheet. Data were then transferred to GraphPad Prism 6 to generate plots.

Supplementary Material

Refer to Web version on PubMed Central for supplementary material.

Acknowledgements

This work was supported by the UC Irvine School of Physical Sciences and the National Science Foundation (CAREER award to J.A.P.) A.C.L. received support from the BEST IGERT program funded by the National Science Foundation (DGE-114–4901). S. H. T was supported by the University of California, Irvine, Undergraduate Research Opportunities Program (UROP) Fellowship under Grant GF10968. We thank Dr. Jennifer Atwood for training and assistance with flow cytometry experiments. The authors wish to acknowledge the support of the Chao Family Comprehensive Cancer Center IFI Flow Cytometry Core Shared Resource, supported by the National Cancer Institute of the National Institutes of Health under award number P30CA062203. The content is solely the responsibility of the authors and does not necessarily represent the official views of the National Institutes of Health. Additional thanks to the members of the Hui, Weiss, Spitale, and Martin labs for reagents and experimental assistance, and all Prescher lab members for helpful discussions.

References

[1]. Dura B, Voldman J, Curr. Opin. Immunol 2015, 35, 23–29. [PubMed: 26050635]

[2]. Pandolfi F, Franza L, Altamura S, Mandolini C, Cianci R, Ansari A, Kurnick JT, Clin. Ther. 2017, 39, 2420–2436. [PubMed: 29203050]

[3]. West J, Newton PK, Proc. Natl. Acad. Sci. USA 2019, 116, 1918–1923. [PubMed: 30674661]

[4]. Shaner NC, Steinbach PA, Tsien RY, Nat. Methods 2005, 2, 905–909. [PubMed: 16299475]

[5]. Kinoshita N, Huang AJY, McHugh TJ, Suzuki SC, Masai I, Kim IH, Soderling SH, Miyawaki A, Shimogori T, iScience 2019, 15, 28–38. [PubMed: 31026667]

[6]. Livet J, Weissman TA, Kang H, Draft RW, Lu J, Bennis RA, Sanes JR, Lichtman JW, Nature 2007, 450, 56–62. [PubMed: 17972876]

[7]. Kim J, Zhao T, Petralia RS, Yu Y, Peng H, Myers E, Magee JC, Nat. Methods 2012, 9, 96–102.

[8]. Tang R, Murray CW, Linde IL, Kramer NJ, Lyu Z, Tsai MK, Chen LC, Cai H, Gitler AD, Engleman E, Lee W, Winslow MM, eLife 2020, 9, e61080. [PubMed: 33025906]

[9]. Pasqual G, Chudnovskiy A, Tas JM, Agudelo M, Schweitzer LD, Cui A, Hacohen N, Victora GD, Nature 2018, 553, 496–500. [PubMed: 29342141]

[10]. Porterfield WB, Prescher JA, Curr. Opin. Chem. Biol. 2015, 24, 121–130. [PubMed: 25461730]

[11]. Ge Y, Chen L, Liu S, Zhao J, Zhang H, Chen PR, J. Am. Chem. Soc. 2019, 141, 1833–1837. [PubMed: 30676735]

[12]. Kim CK, Cho KF, Kim MW, Ting AY, eLife 2019, 8, e43826. [PubMed: 30942168]

[13]. Watson EE, Angerani S, Sabale PM, Winssinger NJ, J. Am. Chem. Soc. 2021, *ASAP*

[14]. Tian L, Yang Y, Wysocki LM, Arnold AC, Hu A, Ravichandran B, Sternson SM, Looger LL, Lavis LD, Proc. Natl. Acad. Sci. USA 2012, 109, 4756–4761. [PubMed: 22411832]

[15]. Jacome D, Northrup JD, Ruff AJ, Reilly SW, Lee IK, Blizard GS, Sellmyer MA, ACS Chem. Biol. 2021, 16, 52–57. [PubMed: 33351606]

[16]. Ng DN, Fromherz P, ACS Chem. Biol. 2011, 6, 444–451. [PubMed: 21235276]

[17]. Walther R, Rautio J, Zelikin AN, Adv. Drug Deliv. Rev. 2017, 118, 65–77. [PubMed: 28676386]

[18]. Porterfield WB, Jones KA, McCutcheon DC, Prescher JA, J. Am. Chem. Soc. 2015, 137, 8656–8659. [PubMed: 26098396]

[19]. Gao W, Xing B, Tsien RY, Rao J, J. Am. Chem. Soc. 2003, 125, 11146–11147. [PubMed: 16220906]

[20]. Senter PD, Springer CJ, Adv. Drug Deliv. Rev. 2001, 53, 247–264. [PubMed: 11744170]

[21]. Zhang X, Li X, You Q, Zhang X, Eur. J. Med. Chem. 2017, 139, 542–563. [PubMed: 28837920]

[22]. Tietze LF, Krewer B, Chem. Biol. Drug Des. 2009, 74, 205–211. [PubMed: 19660031]

[23]. Searle PF, Chen M-J, Hu L, Race PR, Lovering AL, Grove JI, Guise C, Jaberipour M, James ND, Mautner V, Young LS, Kerr DJ, Mountain A, White SA, Hyde EI, Clin. Exp. Pharmacol. Physiol. 2004, 31, 811–816. [PubMed: 15566399]

[24]. Legigan T, Clarhaut J, Tranoy-Opalinski I, Monvoisin A, Renoux B, Thomas M, Le A Pape, S. Lerondel, S. Papot, Angew. Chem. Int. Ed. 2012, 51, 11606–11610.

[25]. Farquhar D, Pan B, Sakurai M, Ghosh A, Mullen CA, Nelson AJ, Cancer Chemother. Pharmacol. 2002, 50, 65–70. [PubMed: 12111114]

[26]. Ghosh A, Khan S, Marini F, Nelson JA, Farquhar D, Tetrahedron Lett. 2000, 41, 4871–4874.

[27]. Bridgewater JA, Springer CJ, Knox RJ, Minton NP, Michael NP, Collins MK, Eur. J. Cancer 1995, 31, 2362–2370.

[28]. Gruber TD, Krishnamurthy C, Grimm JB, Tadross MR, Wysocki LM, Gartner ZJ, Lavis LD, ACS Chem. Biol. 2018, 13, 2888–2896. [PubMed: 30111097]

[29]. Sellmyer MA, Bronsart L, Imoto H, Contag CH, Wandless TJ, Prescher JA, Proc. Natl. Acad. Sci. USA 2013, 110, 8567. [PubMed: 23650381]

[30]. Chao DL, Ma L, Shen K, Nat. Rev. Neurosci. 2009, 10, 262–271. [PubMed: 19300445]

[31]. van der Merwe PA, Dushek O, Nat. Rev. Immunol. 2011, 11, 47–55. [PubMed: 21127503]

[32]. van der Merwe PA, Barclay AN, Trends Biochem. Sci. 1994, 19, 354–358. [PubMed: 7985226]

[33]. Morsut L, Roybal KT, Xiong X, Gordley RM, Coyle SM, Thomson M, Lim WA, Cell 2016, 164, 780–791. [PubMed: 26830878]

[34]. Kopan R, Cell Sci J. 2002, 115, 1095–1097.

[35]. Toda S, McKeithan WL, Hakkinen TJ, Lopez P, Klein OD, Lim WA, Science 2020, 370, 327–331. [PubMed: 33060357]

[36]. Doshi A, Sadeghi F, Varadarajan N, Cirino PC, Crit. Rev. Biotechnol. 2020, 1–20.

[37]. Ausländer S, Fussenegger M, Trends Biotechnol. 2013, 31, 155–168. [PubMed: 23245728]

[38]. Mullick A, Xu Y, Warren R, Koutroumanis M, Guilbault C, Broussau S, Malenfant F, Bourget L, Lamoureux L, Lo R, Caron AW, Pilotte A, Massie B, BMC Biotechnol. 2006, 6, 43. [PubMed: 17083727]

[39]. Eaton RW, Bacteriol J. 1997, 179, 3171–3180.

[40]. Rossi FMV, Kringstein AM, Spicher A, Guicherit OM, Blau HM, Mol. Cell 2000, 6, 723–728. [PubMed: 11030351]

[41]. Vergne-Vaxelaire C, Bordier F, Fossey A, Besnard-Gonnet M, Debard A, Mariage A, Pellouin V, Perret A, Petit J-L, Stam M, Salanoubat M, M.; J. Weissenbach, V. De Berardinis, A. Zaparucha, Adv. Synth. Catal. 2013, 355, 1763–1779.

[42]. O'Reilly C, Turner PD, J. Appl. Microbiol. 2003, 95, 1161–1174. [PubMed: 14632988]

[43]. DeSantis G, Zhu Z, Greenberg WA, Wong K, Chaplin J, Hanson SR, Farwell B, Nicholson LW, Rand CL, Weiner DP, Robertson DE, Burk MJ, J. Am. Chem. Soc. 2002, 124, 9024–9025. [PubMed: 12148986]

[44]. Li Z, Zhu Y, Sun Y, Qin K, Liu W, Zhou W, Chen X, ACS Chem. Biol. 2016, 11, 3273–3277. [PubMed: 27805363]

[45]. Pala Wilgus C, Downing S, Molitor E, Bains S, Pagni RM, Kabalka GW, Tetrahedron Lett. 1995, 36, 3469–3472.

[46]. Luo H, Fan L, Chang Y, Ma J, Yu H, Shen Z, Appl. Biochem. Biotechnol. 2010, 160, 393–400. [PubMed: 18677653]

[47]. Black GW, Brown NL, Perry JJB, Randall PD, Turnbull G, Zhang M, Chem. Commun. 2015, 51, 2660–2662.

[48]. Costello A, Lao NT, Gallagher C, Capella Roca B, Julius LAN, Suda S, Ducrée J, King D, Wagner R, Barron N, Clynes M, Biotechnol J. 2019, 14, e1800219.

[49]. Horbal L, Luzhetskyy A, Metab. Eng. 2016, 37, 11–23. [PubMed: 27040671]

[50]. Jones KA, Li DJ, Hui E, Sellmyer MA, Prescher JA, ACS Chem. Biol. 2015, 10, 933–938. [PubMed: 25643167]

[51]. Gibson DG, Young L, Chuang R-Y, Venter JC, Hutchison CA, Smith HO, Nat. Methods 2009, 6, 343–345. [PubMed: 19363495]

[52]. Jones KA, Porterfield WB, Rathbun CM, McCutcheon DC, Paley MA, Prescher JA, J. Am. Chem. Soc. 2017, 139, 2351–2358. [PubMed: 28106389]

[53]. Carpenter AE, Jones TR, Lamprecht MR, Clarke C, Kang IH, Friman O, Guertin DA, Chang JH, Lindquist RA, Moffat J, Golland P, Sabatini DM, Genome Biol. 2006, 7, R100. [PubMed: 17076895]

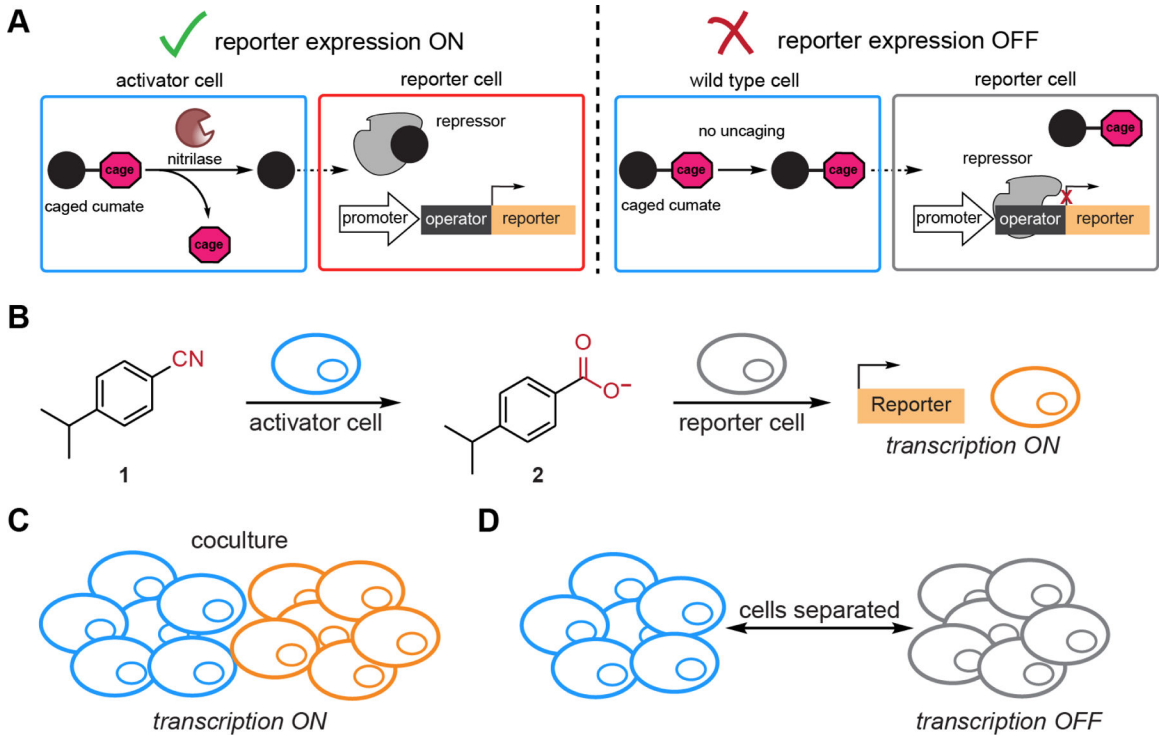

Figure 1.

Proximity-dependent control of gene expression. (A) Nitrilase-expressing cells selectively uncage and release a small molecule activator of gene transcription. Differential gene expression is observed in reporter cells when in the presence of activator cells. (B) Aryl nitrile caged probe is converted to cumate by activator cells. Uncaged cumate is then consumed by reporter cells, inducing gene transcription. (C-D) Target gene expression in populations of reporter cells is modulated by distance. When reporter cells and activator cells are in contact, high numbers of reporter cells express the gene of interest. When reporter cells and activator cells are separated, fewer reporter cells express the gene of interest

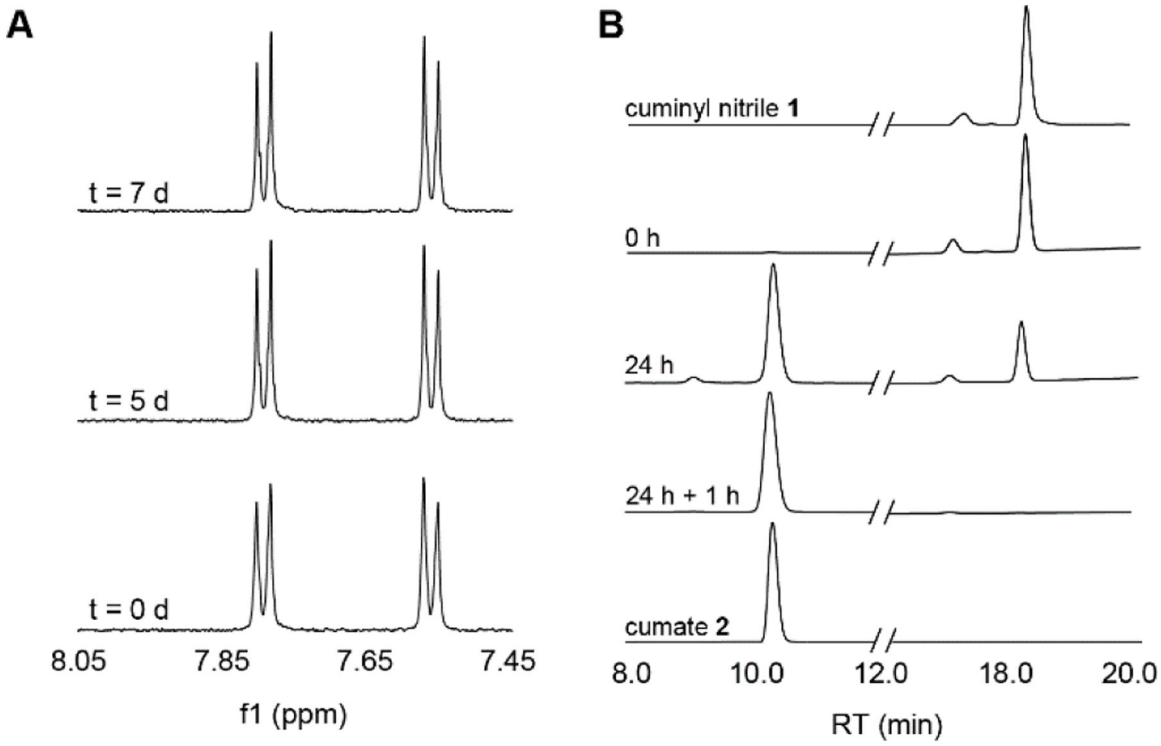

Figure 2.

Cumate can be effectively caged with a nitrile group. (A) Nitrile-caged cumate (**1**, 1 mM) in *d*-PBS (37 °C) was monitored over 7 d by ^{1}H-NMR spectroscopy. (B) Caged cumate **1** (1 mM) was incubated with purified *Rh*NIT and analyzed via HPLC. Complete conversion of **1** to **2** was observed by comparison to known standards (1 mM). For (A)-(B), data are representative of three biological replicates.

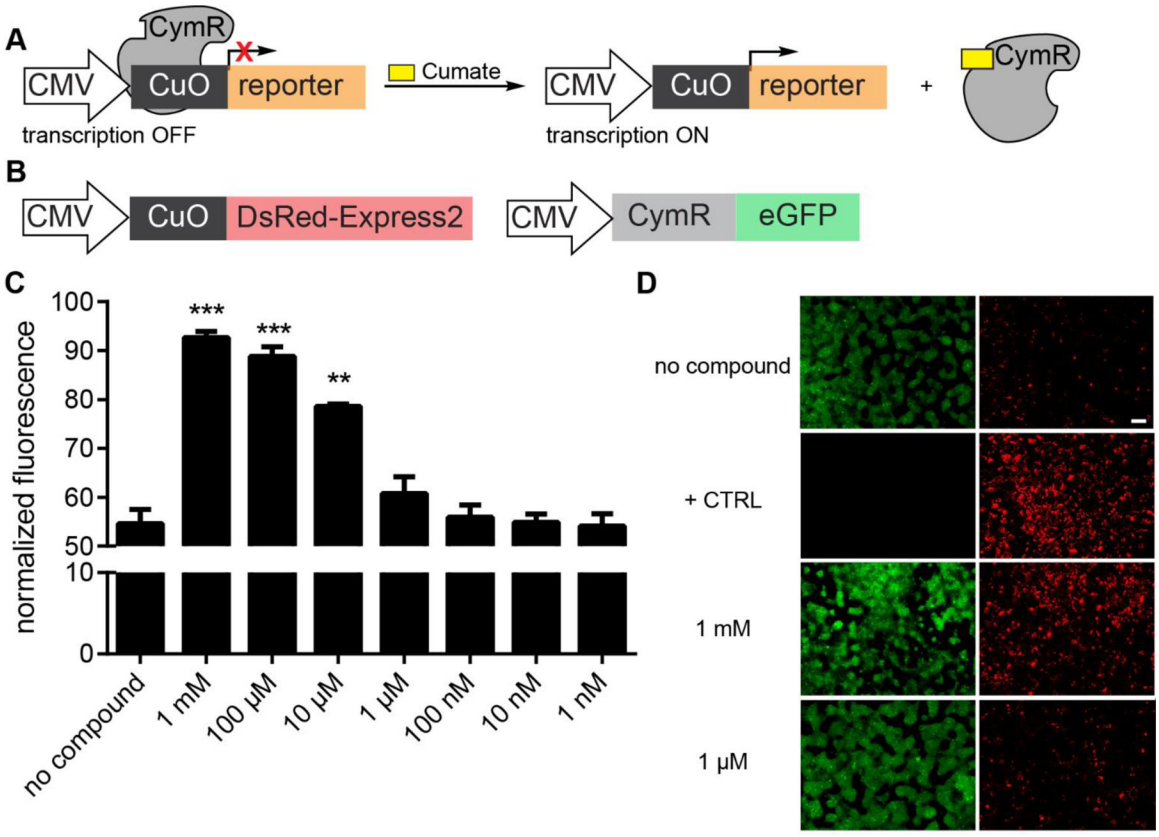

Figure 3.

Cumate genetic switch is operative *in cellulo*. (A) General scheme for inducing reporter gene expression. The CymR repressor binds the CuO operator, blocking transcription of a downstream reporter. CymR is released from the operator upon binding cumate, enabling transcription of the reporter. (B) Constructs for testing the cumate system *in cellulo*. The CuO operator sequence was inserted downstream of a CMV promoter and directly upstream of the gene encoding DsRed. The CymR repressor protein was cloned as a fusion with eGFP. HEK cells stably expressing the repressor were generated via CRISPR-mediated gene insertion. (C) Flow cytometry analysis of CymR-eGFP-expressing cells following transfection of the CuO-DsRed reporter plasmid and cumate (0–1 mM) addition. Error bars represent the standard error of the mean for n = 3 samples. Data are representative of n = 3 biological replicates, ***$p < 0.001$; **$p < 0.01$. (D) Fluorescence microscopy analysis of some samples from (C). CymR-eGFP-expressing cells or HEK cells only (+CTRL) were transfected with the CuO-DsRed reporter plasmid and treated with cumate (0–1 mM). Scale bar = 300 µm.

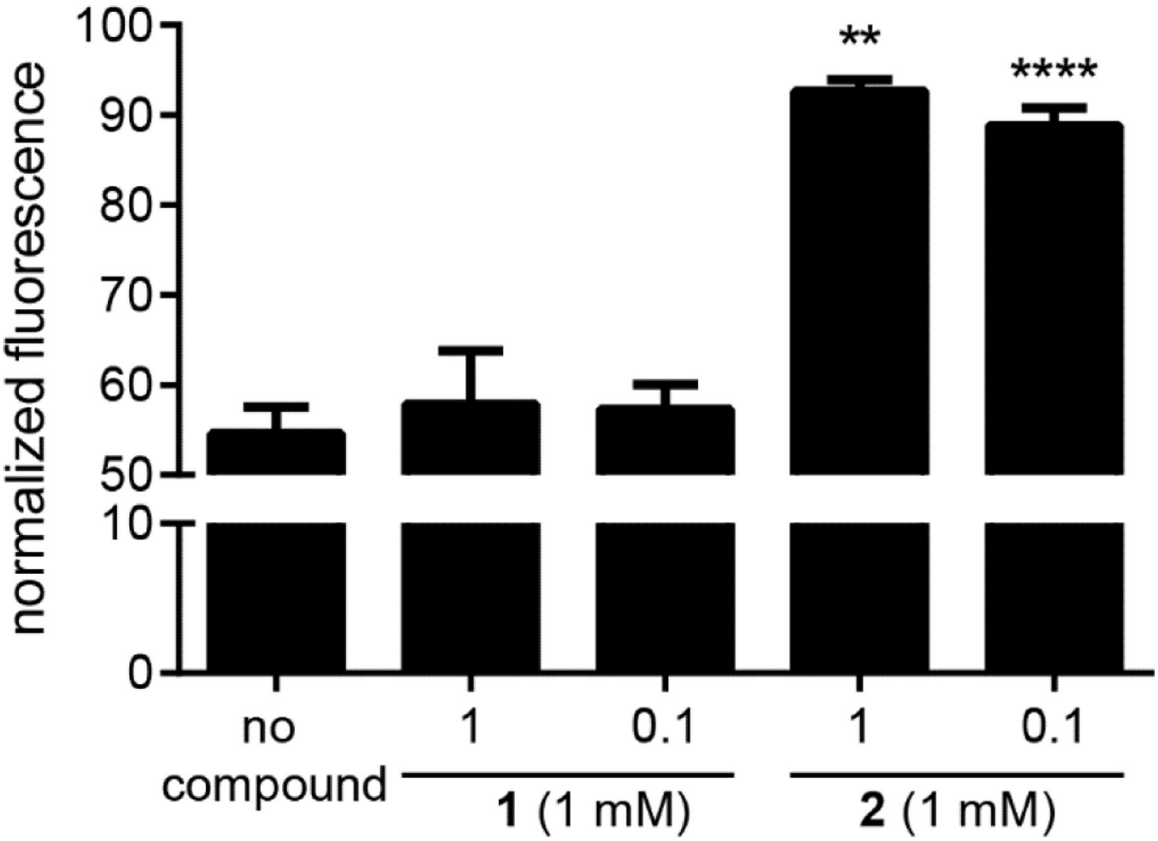

Figure 4.

Caged cumate does not induce gene expression in cells (A) Reporter cells were treated with **1** or **2** and analyzed via flow cytometry. No DsRed expression above background was observed for reporter cells exposed to caged probe **1**. Error bars represent the standard error of the mean for n = 3 samples, ***$p < 0.001$ ** $p < 0.01$. Data are representative of 3 biological replicates.

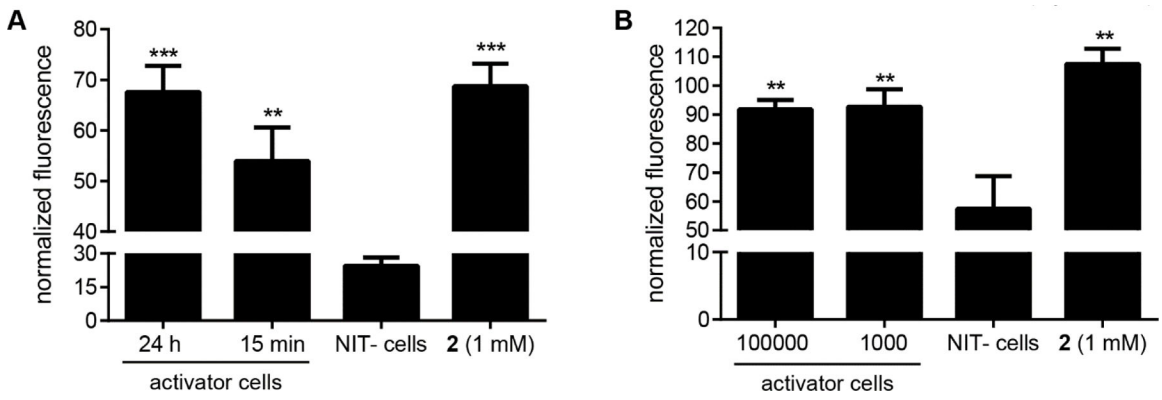

Figure 5.

Caged cumate is rapidly liberated *in cellulo*. (A) eGFP-NIT-expressing activator cells were treated with **1** (1 mM) over 24 h. A negative control was also included wherein HEK cells only (NIT–) were incubated with **1** (1 mM) for 24 h. Media from the cultures was transferred to reporter cells. Reporter cells only were treated with **2** (1 mM) as a positive control. After 3 d, cells were analyzed via flow cytometry. (B) eGFP-NIT-expressing activator cells were plated at different densities and treated with **1** (1 mM) for 15 min. Media was then transferred to reporter cells and analyzed via flow cytometry. Media from HEK cells only (NIT–) or reporter cells treated with **2** (1 mM) directly were used as controls. Robust expression of DsRed was observed with only 1,000 activator cells. Error bars represent the standard error of the mean for n = 3 samples, ***$p < 0.001$; **$p < 0.01$. Data are representative of 3 biological replicates.

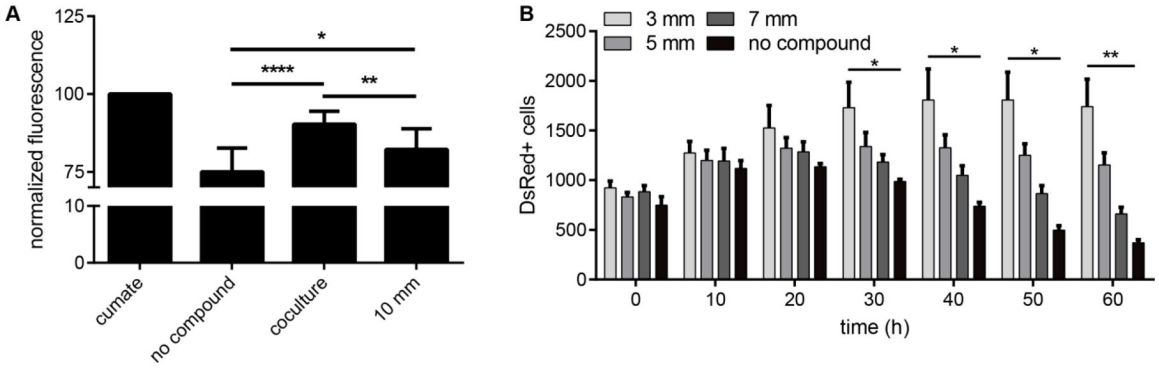

Figure 6.

Caged cumate can report on cellular interactions. (A) CymR reporter cells were transiently transfected with the CuO-DsRed reporter plasmid and plated together with (coculture) or separated from (10 mm) eGFP-*Rt*NIT cells in biocompatible stencils. Stencils were then removed and cells were treated with **1** (1 mM), **2** (1 mM), or no compound prior to flow cytometry analysis. Error bars represent the standard error of the mean for n = 9 samples, ****$p < 0.0001$; ***$p < 0.001$; **$p < 0.01$; *$p < 0.05$. Data are representative of n = 9 biological replicates (B) Cells were prepared as in (A) but separated by distances of 3, 5 or 7 mm. After plating, **1** (10 μM) was added to all samples except the no compound control, and cells were monitored via time lapse microscopy for 60 h. DsRed positive cells were counted using CellProfiler and plotted over time. Error bars represent the standard error of the mean for n = 3 samples, **$p < 0.01$; *$p < 0.05$. Data are representative of 3 biological replicates.